ESR of Co^{2+} in $NH_4NiPO_4 \cdot 6H_2O$

A. Goñi, L. M. Lezama, and T. Rojo
Departamento de Química Inorgánica, Facultad de Ciencias, Universidad del País, Vasco, Apartado 644, 48080 Bilbao, Spain

M. E. Foglio, J. A. Valdivia, and G. E. Barberis
Instituto de Física ''Gleb Wataghin,'' UNICAMP, 13083-970, Campinas, São Paulo, Brazil
(Received 9 July 1997)

Experiments of electron-spin resonance (ESR) were performed on Co^{2+} in single-crystal and powder samples of $NH_4NiPO_4 \cdot 6H_2O$. The angular variation of the resonance field of the crystalline sample can be interpreted in terms of two magnetically nonequivalent sites related by a symmetry operation. From the fitting of the ESR data, the spin-Hamiltonian parameters are determined. A theoretical analysis of these results is presented. [S0163-1829(98)00701-2]

I. INTRODUCTION

Ni(II) hydrated phosphates are very interesting because of their physicochemical properties,[1] generated by the great diversity of their crystal structures. The structural model of these phases changes as a function of the ratio $Ni:PO_4$ in their composition. It is observed that when there are several water molecules per Ni atom in the formula, most of the positions in the coordination sphere of the metal are occupied by those molecules. This gives place to three-dimensional (3D) structures, connected through hydrogen bridges,[2,3] as it is the case with the compound discussed here.

$NH_4NiPO_4 \cdot 6H_2O$ presents a 3D structure formed by a complicated scheme of hydrogen bonds, established by the water molecules and the ammonia groups.[4] The $Ni[OH_2]_6$ octahedra are fairly regular, with Ni-O mean distance 2.055(3) Å, and a O-Ni-O mean angle of 91.8(5)°. The PO_4 tetrahedra show a high local symmetry, with a P-O mean distance of 1.535(5) Å, and O-P-O mean angles of 109.6°. The NH_4^+ tetrahedra are quite regular, too. They present mean distances of 0.88 Å and mean H-N-H angles of 109(3)°. There are two crystallographically equivalent $Ni[OH_2]_6$ sites related by the symmetry operation $(1/2-x, -y, 1/2+z)$ (see Fig. 1). However, under the application of a magnetic field, these two sites are not equivalent, and the magnetic group of the crystal has less symmetry operations than the space group.

The local symmetry of the nickel (II) ions is near cubic as stated above, and the electron-spin resonance (ESR) of resonant impurity ions that substitute the Ni in the lattice is a powerful technique to analyze the environment of this ion. The Co^{2+} $(3d^7)$ is very convenient for this purpose, because it has a very strong spin-orbit interaction, its ground state in cubic symmetry is an isotropic Kramers doublet, and it becomes very anisotropic with small changes in the local electric crystal field. The ESR experiments make evident the difference between the two magnetically nonequivalent Ni sites that are present in the structure of $NH_4NiPO_4 \cdot 6H_2O$.

The main objective of this work, is thus to present ESR measurements in single crystals and powder samples of $NH_4NiPO_4 \cdot 6H_2O$, doped with a low concentration (0.1%) of Co^{2+}. The experimental data are empirically analyzed with a spin Hamiltonian. A theoretical analysis with a simple model shows that a fairly good agreement with this empirical spin Hamiltonian is obtained by employing a perturbation calculation that includes the crystal field up to first order only.

II. EXPERIMENTAL DETAILS

A. Materials

$NH_4NiPO_4 \cdot 6H_2O$:0.1% Co^{2+} samples were synthesized by mixing $NiCl_2 \cdot 6H_2O$ and H_3PO_4 in a water solution in a proportion of 1:40, at room temperature.[4] The Co^{2+} doping was obtained substituting 0.1 mol of $NiCl_2 \cdot 6H_2O$ by $CoCl_2 \cdot 6H_2O$. The pH of the solution obtained was increased up to 12 by addition of NH_4OH as needed. The product was slowly evaporated during one week, and the slow evaporation of the ammonia favored the formation of

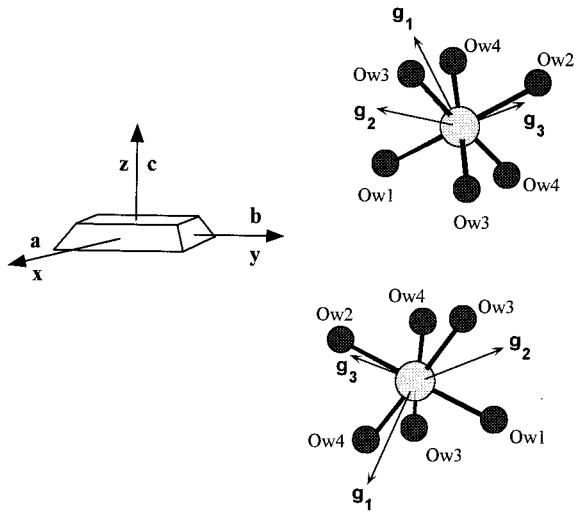

FIG. 1. Geometrical representation of the two Co^{+2} sites in $NH_4NiPO_4 \cdot 6H_2O$. The experimental coordinate system is represented with respect to the orthorhombic crystal axes. The principal crystal directions are drawn within a polyhedron that is shaped as the growing crystal habit.

the desired compound. Recrystallization was necessary to obtain single crystals that are adequate for the ESR measurements. Thermogravimetric measurements and x-ray diffraction were carried on the samples and, within the experimental errors, no impurities were observed. Oscillation and Weissenberg photographs were carried out to determine the relationships between the crystallographic axes and the external morphology of the crystals. The crystals are elongated along the *a* axis, as can be seen in the drawing of the crystal habit in Fig. 1.

B. ESR

The ESR spectra were recorded at the *X* band on a Bruker ESP300 spectrometer equipped with a standard OXFORD helium continuous-flow cryostat. The magnetic field was measured with a Bruker ER035M NMR Gaussmeter. The frequency inside the cavity was measured with a Hewlett-Packard 5352B microwave frequency counter. Powder and single-crystal spectra were recorded at 4.2 K. A single crystal of $NH_4NiPO_4 \cdot 6H_2O$:0.1% Co^{2+}, with a size of $0.23 \times 0.11 \times 0.14$ mm^3, was oriented through Weissenberg photographs and glued to a cleaved KCl sample holder with the *a*, *b*, and *c* crystal directions along its *x*, *y*, and *z* orthogonal axes, respectively (see Fig. 1). The sample holder was connected to an L-shaped quartz rod and rotated with respect to the applied magnetic field using a one axis Bruker goniometer with 1/8° resolution. ESR spectra were recorded rotating the crystal around the *x*, *y*, and *z* axes, with 5° intervals along 180° in each plane. The orientation of the magnetic field within the *zx* and *zy* planes was determined from the ESR data considering the known crystal symmetry. The orientation of the magnetic field in the *xy* plane was accurately defined by matching the angular variation of the spectra in this plane to those obtained in the other two planes.

III. RESULTS AND ANALYSIS

Figure 2 shows the ESR spectra of the single-crystal sample measured at 4.2 K, for three selected directions of the magnetic field. The spectra consist of two octets of resonance lines; those octets are due to the allowed transitions for $\Delta S_z = \pm 1$, $\Delta I_z = 0$ corresponding to the hyperfine interaction between the effective spin $\vec{S} = 1/2$ of the cobalt and the real nuclear spin ($I = 7/2$) of ^{59}Co (100% abundant).

Figure 3 shows the angular variation of the resonance field of the ESR lines in the (100), (010), and (001) planes. Both the angular variation and its symmetry clearly show two magnetically nonequivalent sites related by a C_2 operation about the *c* crystal axis, which is the point operation that relates the two centers. The actual spectra show eight well-resolved hyperfine lines along some directions for each site; but the reduction of the hyperfine interaction causes the collapse of them in other directions (see Fig. 2). The point-group symmetry for the Ni^{2+} ion (and the Co^{2+} substituting them) is Cs, and the appropriate spin Hamiltonian for $\vec{S} = 1/2$ and $\vec{I} = 7/2$ is therefore[6]

$$\hat{H} = \mu_B \mathbf{H} \cdot \mathbf{g}_1 \cdot \mathbf{S}_1 + \mu_B \mathbf{H} \cdot \mathbf{g}_2 \cdot \mathbf{S}_2 + \mathbf{S}_1 \cdot \mathbf{A}_1 \cdot \mathbf{I}_1 + \mathbf{S}_2 \cdot \mathbf{A}_2 \cdot \mathbf{I}_2, \quad (1)$$

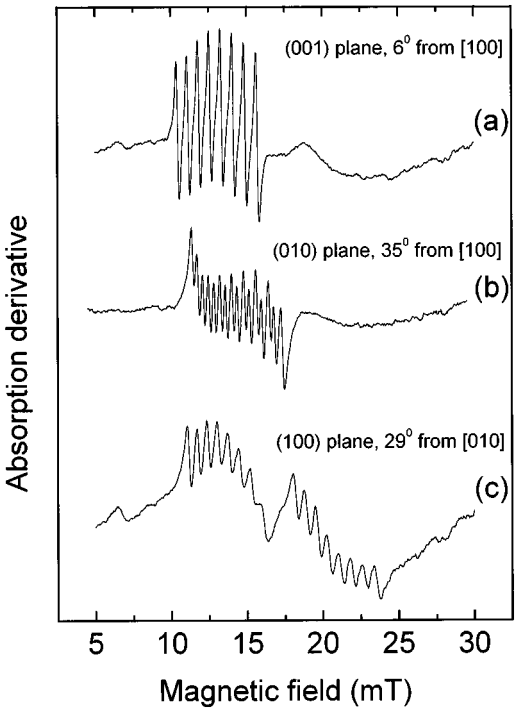

FIG. 2. Three Co^{+2} ESR spectra selected for directions of the magnetic field that show the spectra properties as described in the text.

where $\mathbf{g}_1$and $\mathbf{g}_2$ are the gyromagnetic tensors and $\mathbf{A}_1$ and $\mathbf{A}_2$ the hyperfine tensors for each site. **H** is the applied magnetic field, and μ_B is the Bohr magneton. As a first approximation, the ESR data were used to calculate the **g** and **A** tensors by Schonland's method,[5] and the obtained parameters were used as preliminary information for the subsequent calculation. The resonant field for each transition was obtained exactly, within the machine error, by diagonalizing numerically the 16×16 matrix corresponding to each of the sites in Eq. (1), and obtaining the field self-consistently. These fields were the input to a least-squares fitting program, treating the **g**'*s* and **A**'*s* values as adjusting parameters. All the experimental data of the three planes were fed in the program, and the solid lines in Fig. 3 are the best fitting of the data using Eq. (1). Figure 1 shows the relative orientation of the principal *g*

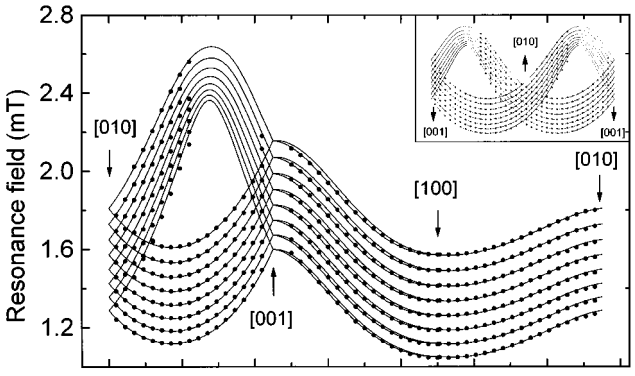

FIG. 3. Angular variation of Co^{+2} in $NH_4NiPO_4 \cdot 6H_2O$ spectra, in the three experimental planes. The principal directions in these planes are indicated in the figure. The solid lines are the best fit to Eq. (1), and the fitting parameters are given in Table I.

TABLE I. Spin-Hamiltonian parameters for Co^{2+} in $NH_4NiPO_4 \cdot 6H_2O$ at 4.2 K.

		$\cos(\theta_1)$	$\cos(\theta_2)$	$\cos(\theta_3)$
g_1	4.9091	−0.26072	−0.55762	0.78809
g_2	5.1389	0.96461	−0.11704	0.23630
g_3	2.6680	−0.03953	0.82180	0.56840
	$\times 10^{-4}$ cm^{-1}	$\cos(\theta_1)$	$\cos(\theta_2)$	$\cos(\theta_3)$
A_1	160.17	−0.20229	−0.58951	0.78202
A_2	178.76	0.97741	−0.07163	0.19884
A_3	44.37	−0.06120	0.80458	0.59068

values for both Co^{2+} sites. Table I gives the spin-Hamiltonian parameters obtained by this procedure.

Figure 4 shows the ESR spectra of a powdered sample. The simulated spectra in it were obtained with the fitted parameters in Table I, considering the powder as a great number of crystallites oriented at random.

IV. THEORETICAL DISCUSSION

In this compound the Co^{2+} ions are coordinated by six O(w) in fairly regular octahedra.[4] Assuming that the position of the six oxygen nearest to the Co^{2+} are in the same positions as those of the nickel compound,[4] and taking the average of their positions as the center of the octahedron, we choose two of the O and use them to determine an orthogonal system of axis. In the new system the x axis goes through the position of one of those two O, and the z axis is perpendicular to the plane determined by the two O and the center of the octahedron. The direction cosines of these axes with respect to the orthorhombic axis of the crystal are given in Table II. The average distance of the six O with respect to the new axes origin is $\overline{R} = 2.0531\overline{A}$, and we can define a regular octahedron with the six vertices placed along the

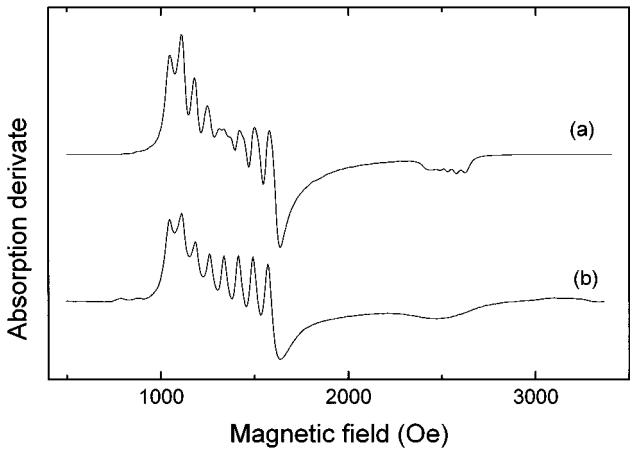

FIG. 4. Experimental (a) and simulated (b) powder spectra of Co^{+2} in $NH_4NiPO_4 \cdot 6H_2O$. This last was obtained using the parameters in Table I, and a powder program. The slight differences are due to the fact that we did not consider the angular variation of the linewidths in the simulation.

TABLE II. The cosines between the orthorhombic axes of the crystal $b\{a,b,c\}$ and the new axes $j = x,y,z$ fixed to the octahedron, as discussed in the text.

Axes	**a**	**b**	**c**
$j=$**x**	0.7328	− 0.3099	− 0.6058
$j=$**y**	−0.00048	0.8900	− 0.4559
$j=$**z**	0.6804	0.3344	0.6521

axes at a distance $\pm\overline{R}$ from the origin. From any displacement of the six O with respect to the vertices of this regular octahedron we can find[9,10] the corresponding normal coordinates Q_j of the seven ion-complex, formed by the Co and the six nearest O, that are invariant against inversion. These are separated in the three sets $\{Q_1\}$, $\{Q_2,Q_3\}$, and $\{Q_4,Q_5,Q_6\}$, and the corresponding Q_j transform, respectively, like the basis of the irreducible representations A_1, E, and T_2 of the cubic group, as given in Table II of Ref. 11. These coordinates will be employed below to model the crystal field that gives the experimental g tensor, and the normal coordinates obtained from the position of the O crystallographically determined[4] in the Ni compound are shown in the first row of Table III.

The ^4F ground state of isolated Co^{2+} ($3d^7$) in a purely octahedral crystal field splits into two orbital triplets $^4T_1$, $^4T_2$ and one orbital singlet $^4A_2$. Spin-orbit effects partially lift the degeneracy of the $^4T_1$ triplet into one Γ_6, two Γ_8, and one Γ_7 subspaces, and the resonance for the lowest doublet (Γ_6) is isotropic with $g=4.33$.[8] The addition of lower symmetry crystal fields produces further splitting of the $^4T_1$ triplet, giving six Kramer's doublets, and in most cases it is found that the trace of the g tensor is close to the cubic isotropic value[7]; in the present case the average g is 4.2387. To understand this value we first consider the Co^{2+} in a cubic symmetry, showing later that crystal fields of lower symmetry do not change this value in our approximation.

In the lowest order one obtains g from the matrix elements of the Zeeman term in the Γ_6 subspace of the $^4T_1$ ground triplet. The matrix elements of the orbital angular momentum **L** within a T_1 subspace are proportional to those of a P term, but one should note that the excited term ^4P is also of the $^4T_1$ symmetry, and is mixed by the cubic field

TABLE III. The symmetrical normal coordinates of the complex formed by the Co and the six O with respect to the regular octahedron defined in the text. Row 1 gives the values calculated from the O positions determined crystallographically. Row 2 gives the values that would reproduce the experimental g tensor for the point charge model. Row 3 gives a number proportional to the ratio of the normal coordinates obtained from the g tensor divided into those obtained from the A tensor.

	Q_2	Q_3	Q_4	Q_5	Q_6
1	−0.03840	0.02497	0.01417	0.06542	−0.01275
2	0.01092	0.00305	0.16028	−0.22616	−0.14710
3	1.60	845	2.04	1.77	1.99

with the $^4T_1$ of the ground ^4F term. If we indicate two states of ^4F and ^4P with ϕ_i and ϕ_i', respectively, such that they transform in the same way under the cubic group, the states of the ground $^4T_1$ will be of the form $a\phi_i+b\phi_i'$. The values of the constants a and b can be obtained[12,13] from the Racah parameter B and the crystal-field parameter Dq, that take the values 918 and 840 cm^{-1}, respectively in the Ni compound:[4] with these values one obtains $a=0.9853$ and $b=-0.1707$, and the proportionality constant of the angular momentum is

$$\alpha=-1.5a^2+b^2=-1.4271.$$

Two further effects should be considered in the calculation of the isotropic g tensor. One is the second-order contribution of the $^4T_2$ states, that are separated by $\Delta'=-15B-6Dq=7302$ cm^{-1} from the ground $^4T_1$ states, and the other is the covalency between the Co and the neighboring O, described by several covalence factors,[7,12] that reduce the matrix elements of the orbital angular momentum and of the spin-orbit interaction. Using a single k_0 for all these factors one obtains the expression for the g factor in a cubic field:

$$g=\frac{5}{3}g_e-\frac{2}{3}\alpha k_0+2\left(\frac{\sqrt{15}}{2}a+b\right)^2(k_0)^2\frac{|\lambda|}{\Delta'}, \qquad (2)$$

where $\lambda=-180$ cm^{-1} is the Co^{2+} spin-orbit interaction. With the parameters employed, this isotropic g tensor coincides with the trace of the experimental one when $k_0=0.84$. When one employs the parameters of Co:MgO, viz. $B=815$ cm^{-1} and $Dq=905$ cm^{-1}, the following values are obtained: $a=0.9811$, $b=-0.1933$, $\alpha=-1.4063$, $\Delta'=7953$ cm^{-1}, and $k_0=0.86$. These values are not very different from those obtained with the Ni parameters B and Dq.

To analyze further the experimental g tensor, one could try and find crystal-field values that would reproduce the measured results, and a study of this type was presented by Abragam and Pryce for the cobalt Tutton salts.[14] To simplify the study we present a model that describes all the crystal fields acting on Co as originating in the crystal field of the six nearest O located at the vertices of a deformed octahedron, obtained by displacement of the vertices of the regular octahedron introduced at the beginning of this section. If one neglects the mixing of other configurations into the ground configuration $(3d)^7$, it is sufficient to keep only the part of the crystal field V that is even against inversion. We could then write $V=\Sigma_{i=1}^{7}V(\mathbf{r}_i)$, where $V(\mathbf{r})$ would be the sum of products of only two or four components of the electronic coordinates $\mathbf{r}$. Within our model, one could then write[9]

$$V(\mathbf{r})=\sum_j Q_jV_j(\mathbf{r}), \qquad (3)$$

where the Q_j and $V_j(\mathbf{r})$ transform like the same partners of irreducible representations of the octahedral group.[11] As the $V_j(\mathbf{r})$ must be even against inversion, the Q_j must have the same property, and only the six Q_j with $j=1,6$ discussed at the beginning of this section would appear in Eq. (3). In the following we shall not consider the identical representation A_1 because it does not modify the g tensor. The useful $V_j(\mathbf{r})$ are then

$$V_2(\mathbf{r})=A(x^2-y^2)+B(x^4-y^4),$$

$$\sqrt{3}V_3(\mathbf{r})=A(3z^2-r^2)+B(2z^4-x^4-y^4), \qquad (4)$$

and

$$V_4(\mathbf{r})=Czy+E(z^3y-y^3z),$$

$$V_5(\mathbf{r})=Cxz+E(x^3z-z^3x),$$

$$V_6(\mathbf{r})=Cxy+E(x^3y-y^3x). \qquad (5)$$

For a point-charge model,[9] the constants are given by

$$A=\frac{1}{4}ee_{\text{eff}}(18R^{-4}-75R^{-6}r^2), \quad B=175ee_{\text{eff}}/8R^6,$$

$$C=ee_{\text{eff}}(-6R^{-4}+15R^{-6}r^2), \quad E=-35ee_{\text{eff}}/2R^6, \qquad (6)$$

where e_{eff} is an effective charge associated with the O.

To study the effect on the g tensor of the $V(\mathbf{r})$ given in Eq. (3), we shall employ second-order perturbation theory, using both $V(\mathbf{r})$ and the Zeeman term $H_Z=(g_e\mathbf{S}+\mathbf{L})\cdot\mathbf{H}$ as perturbation. The change in the g tensor is then given by

$$\delta g=\frac{2}{3}(g_e+\alpha)\frac{\mu_B}{\Delta}\{-C_E[\sqrt{3}Q_2(S_xH_x-S_yH_y)+Q_3(3S_zH_z-\mathbf{S}\cdot\mathbf{H})]+C_T[Q_4(S_zH_y+S_yH_z)+Q_5(S_xH_z+S_zH_x)+Q_6(S_xH_y+S_yH_x)]\}, \qquad (7)$$

where μ_B is the Bohr magneton and Δ is the splitting between the Γ_6 doublet and the lowest Γ_8 quadruplet in the octahedral symmetry, given by[12]

$$\Delta=1.5(-1.5a^2+b^2)k_0\lambda-\frac{33}{20}\left(\frac{\sqrt{15}}{2}a+b\right)^2k_0^2\frac{\lambda^2}{\Delta'}. \qquad (8)$$

The constants C_E and C_T can be obtained by calculating a single matrix element in each case:

$$C_E=-\frac{1}{2}\langle T_1z|\sum_j V_3(\mathbf{r}_j)|T_1z\rangle \qquad (9)$$

and

$$C_T=\langle T_1x|\sum_j V_3(\mathbf{r}_j)|T_1y\rangle, \qquad (10)$$

where the $\{|T_1x\rangle,|T_1y\rangle,|T_1z\rangle\}$ are a basis of the ground $^4T_1$ that transforms like the coordinates $\{x,y,z\}$ under the octahedral group.

The expression in Eq. (7) corresponds to deformations from a cubic environment, and one should then compare this formula with the experimental g tensor in the axis of the regular octahedron defined in Table II, which is given in Table IV, but it is first necessary to determine C_E and C_T. One obtains with Eqs. (3)–(6)

TABLE IV. The components of the experimental g tensor, referred to the octahedron axes $j=x,y,z$, after subtraction of the isotropic tensor $g=4.2387$.

Axes	$g_{j,x}$	$g_{j,y}$	$g_{j,z}$
$j=\mathbf{x}$	−0.1306	0.6354	0.9769
$j=\mathbf{y}$	0.6354	0.1809	−0.6923
$j=\mathbf{z}$	0.9769	−0.6923	−0.0503

$$C_E=\frac{ee_{\rm eff}}{\overline{R^2}}\left\{(1.4846-1.7815a^2+1.7815ab-0.4454b^2)\frac{\langle r^2\rangle}{\overline{R^2}}+(-0.1718+0.6873a^2-0.6873ab+0.1718b^2)\frac{\langle r^4\rangle}{\overline{R^4}}\right\} \tag{11}$$

and

$$C_T=\frac{ee_{\rm eff}}{\overline{R^2}}\left\{(0.0857a^2-1.3714ab+1.2b^2)\frac{\langle r^2\rangle}{\overline{R^2}}+(-0.7143a^2-0.2381ab)\frac{\langle r^4\rangle}{\overline{R^4}}\right\}. \tag{12}$$

The averages $\langle r^2\rangle=1.251$ and $\langle r^4\rangle=3.655$ (atomic units) have been calculated with Hartree-Fock functions,[13] but we can obtain $e_{\rm eff}\langle r^4\rangle$ from the cubic field parameter Dq employing the relation

$$Dq=-\frac{1}{6}\frac{ee_{\rm eff}}{\overline{R}}\frac{\langle r^4\rangle}{\overline{R^4}} \tag{13}$$

valid for the point-charge model. To find $e_{\rm eff}\langle r^2\rangle$ we shall assume that $\langle r^2\rangle/\sqrt{\langle r^4\rangle}=0.6544$, i.e., equal to the corresponding ratio obtained from the calculated values. Taking the B and Dq of the Ni compound and using for the remaining parameters those discussed in the text, one finds $C_E=6508\ \text{cm}^{-1}/\text{Å}$ and $C_T=-3414\ \text{cm}^{-1}/\text{Å}$, while for the Co:MgO values one finds $C_E=6821\ \text{cm}^{-1}/\text{Å}$ and $C_T=-3932\ \text{cm}^{-1}/\text{Å}$. The difference is not critical, and we shall use the Ni values in the remaining of the discussion.

It is now possible to compare Eq. (7) with Table IV, and one immediately obtains values of the normal coordinates that would reproduce the experimental g tensor when substituted in that equation. These values are given in the second line of Table III, and it is clear that they are rather different from the values calculated from the crystallographic position of the O in the Ni compound. There are two alternative explanations for this result: either the O around the Co impurity are in different positions than in the Ni compound, or the model is not adequate. In the absence of experimental evidence to check the first alternative, we shall discuss possible modification to the model employed above. Instead of the point-charge model we could use a model with dipoles, all ''directed away from the central ion.''[9] This model gives the same potential of Eqs. (3)–(5) but with different expression for the constants A,B,C,E. Within each irreducible representations E and T_2, the normal coordinates necessary to reproduce the g tensor would then be proportional to those obtained with the point-charge model, as only the values of C_E and C_T would change in this model, so that both the charge and dipole models would give essentially the same results. A more complicated model, either involving the change in the direction of the dipoles, or even considering the extended charges of the ligands, would increase very much the difficulty of the calculation. We should then remain with the point-charge model, but only as a means to obtain a fairly simple crystal field that would be sufficient to explain the experimental g tensor. This crystal field is the $V(\mathbf{r})$ of Eq. (3) given in the axes of the regular octahedron defined in Table II with the Q_j given in the second row of Table III. The agreement is perfect because there are as many free normal coordinates as δg components, but the point-charge model employed should not be taken too seriously.

TABLE V. The components of the experimental A tensor (given in cm^{-1}), referred to the octahedron axes $j=x,y,z$, after subtraction of the isotropic tensor $A=12\,780\ \text{cm}^{-1}$.

Axes	$A_{j,x}$	$A_{j,y}$	$A_{j,z}$
$j=\mathbf{x}$	−970	3200	5510
$j=\mathbf{y}$	3200	970	−3390
$j=\mathbf{z}$	5510	−3390	0

Although we have not analyzed the hyperfine tensor in detail, we can extract some information from its experimental value. As seen from Table I, the principal axes of the two tensors g and A do not exactly coincide, but are fairly close together. As with the g tensor, we have expressed the δA tensor in the axes of the regular octahedron discussed above, and the corresponding values are given in Table V. One can show[15] that the δA is described by an expression similar to that of the δg [cf. Eq. (7)] with the component of $\mathbf{I}$ taking the place of the components of $\mathbf{H}$, but we have not explicitly calculated the coefficients equivalent to the C_E and C_T. Nevertheless, by the same method employed with the g tensor one can obtain quantities Q_j' proportional to the Q_j, and then calculate the ratio of the Q_j given in the second row of Table III to the corresponding Q_j' obtained from the A tensor. These ratios are given in the third row of Table III, and those corresponding to Q_j of the same irreducible representation should be equal if the theory were strictly true. The enormous value of the ratio corresponding to Q_3 is not significant, because the value derived from the A tensor is zero within the experimental error, and one can therefore not draw any conclusions from the pair $\{Q_2,Q_3\}$. On the other hand, the three ratios corresponding to $\{Q_4,Q_5,Q_6\}$ are fairly close to the same value, and they show that the crystal fields that result from the present treatment are fairly consistent with the available experimental results.

In the present calculation we have neglected the effect of the $^4T_2$ triplet, that contributes to δg in third-order perturbation (our calculation would be of the second-order). This effect was calculated by Tucker[13] who obtained contributions that are about 6% of the second-order contribution for the T_2 deformation and about 13% for the E deformation, and would therefore not alter substantially our conclusions.

ACKNOWLEDGMENTS

We would like to acknowledge financial support from the Basque Government, as well as from the Brazilian agencies FAPESP and CNPq . G.E.B. is grateful to the Universidad del País Vasco for its hospitality. This work was done (in part) in the frame of the Associate Membership Program of the International Centre for Theoretical Physics, Trieste, Italy (M.E.F. and G.E.B.).

[1] T. Kanazawa, *Inorganic Phosphate Materials* (Elsevier, Tokyo, 1993).

[2] A. Jouini, M. Dabbabi, and A. Durif, J. Solid State Chem. **60**, 6 (1985).

[3] M. Berraho, C. R'Kha, A. Vegas, and F. Rafig, Acta Crystallogr., Sect. C: Cryst. Struct. Commun. **48**, 1350 (1992).

[4] A. Goñi, J. L. Pizarro, L. M. Lezama, G. E. Barberis, M. I. Arriortua, and T. Rojo, J. Mater. Chem. **6**, 412 (1996).

[5] C. H. P. Poole and H. A. Farach, *The Theory of Magnetic Resonance* (Wiley, New York, 1972).

[6] A. Abragam and B. Bleaney, *EPR of Transition Ions* (Clarendon, Oxford, 1970).

[7] M. Tinkham, Proc. R. Soc. London, Ser. A **236**, 549 (1956).

[8] A. Abragam and B. Bleaney, *EPR of Transition Ions* (Ref. 6), Sec. 7.14, p. 447.

[9] J. H. Van Vleck, J. Chem. Phys. **7**, 72 (1939).

[10] The definitions of the normal coordinates Q_j we employ in this work are slightly different from those in Ref. 9.

[11] G. F. Koster, J. O. Dimmock, R. G. Wheeler, and H. Stats, *Properties of the Thirty-Two Point Groups* (M.I.T. Press, Cambridge, Massachusetts, 1963).

[12] L. T. Peixoto and M. E. Foglio, Rev. Bras. Fis. **13**, 564 (1983).

[13] E. B. Tucker, Phys. Rev. **143**, 264 (1966).

[14] A. Abragam and M. H. L. Pryce, Proc. R. Soc. London, Ser. A **206**, 173 (1951).

[15] M. E. Foglio, Ph.D. thesis, University of Bristol, Bristol, England, 1962.